# Production, purification, crystallization and preliminary X-ray structural studies of adeno-associated virus serotype 5

Michael DiMattia,[a] Lakshmanan Govindasamy,[a] Hazel C. Levy,[a] Brittney Gurda-Whitaker,[a] Amy Kalina,[a] Erik Kohlbrenner,[b] John A. Chiorini,[c] Robert McKenna,[a] Nicholas Muzyczka,[d] Sergei Zolotukhin[b] and Mavis Agbandje-McKenna[a]*

[a]Department of Biochemistry and Molecular Biology, McKnight Brain Institute, Center for Structural Biology, University of Florida, Gainesville, FL 32610, USA, [b]Division of Cell and Molecular Therapy, University of Florida, Gainesville, FL 32610, USA, [c]GTTB, NIDCR, National Institutes of Health, Bethesda, MD 20892, USA, and [d]Department of Molecular Genetics and Microbiology and Powell Gene Therapy Center, College of Medicine, University of Florida, Gainesville, FL 32610, USA

Correspondence e-mail: mckenna@ufl.edu

Adeno-associated virus serotype 5 (AAV5) is under development for gene-therapy applications for the treatment of cystic fibrosis. To elucidate the structural features of AAV5 that control its enhanced transduction of the apical surface of airway epithelia compared with other AAV serotypes, X-ray crystallographic studies of the viral capsid have been initiated. The production, purification, crystallization and preliminary crystallographic analysis of empty AAV5 viral capsids are reported. The crystals diffract X-rays to beyond 3.2 Å resolution using synchrotron radiation and belong to the orthorhombic space group $P2_12_12_1$, with unit-cell parameters $a = 264.7$, $b = 447.9$, $c = 629.7$ Å. There is one complete $T = 1$ viral capsid per asymmetric unit. The orientation and position of the viral capsid in the asymmetric unit have been determined by rotation and translation functions, respectively, and the AAV5 structure determination is in progress.

1. Introduction

Recent years have seen increased potential for the utilization of adeno-associated viruses (AAVs), members of the *Dependovirus* genus of the ssDNA *Parvoviridae* family, as recombinant vectors for gene therapy (Flotte & Carter, 1995). 11 distinct AAV serotypes (AAV1–11) have been sequenced and studies show that each virus has unique cellular transduction characteristics (Burger *et al.*, 2004; Davidson *et al.*, 2000; Gao *et al.*, 2002; Kaludov *et al.*, 2001; Mori *et al.*, 2004; Rabinowitz *et al.*, 2002; Walters *et al.*, 2001). In addition, mutagenesis, cell-binding and transduction studies show that the capsid-protein amino-acid sequence plays a central role in the observed tissue-recognition and transduction-efficiency disparities (Kern *et al.*, 2003; Opie *et al.*, 2003). These observations and the goal of enhancing the efficacy of AAV gene-therapy applications by viral capsid modifications for specific cell/tissue targeting have created a necessity for an understanding of their capsid structures and inter-actions with cell-surface ligands.

AAV5, one of the most divergent serotypes when compared with the more widely studied AAV2 (Bantel-Schaal *et al.*, 1999), binds and infects the apical surface of human airway epithelia more efficiently than AAV2 by factors of 20 and 50 *in vivo* and *in vitro*, respectively (Walters *et al.*, 2001). This property has resulted in the utilization of recombinant AAV5 capsids carrying the gene for the cystic fibrosis transmembrane conductance regulator for gene-therapy applications aimed at the treatment of cystic fibrosis. The AAV capsid contains 60 copies (in total) of three overlapping viral proteins (VP), VP1–VP3, translated from the same mRNA. Amino acids in the overlapping VP region mediate AAV5's transduction of epithelial cells through interaction with sialic acid, rather than the heparin sulfate utilized by AAV2 for broad-range cellular transduction (Davidson *et al.*, 2000; Kaludov *et al.*, 2001; Walters *et al.*, 2001). In the crystal structures of AAV2 and AAV4, only the overlapping C-terminal polypeptide region is ordered, with $T = 1$ icosahedral symmetry, and shows differences in regions that control AAV2 receptor attachment and antigenicity (Xie *et al.*, 2002; L. Govindasamy, E. Padron, N. Kaludov, R. McKenna, N. Muzyczka, J. Chiorini & M. Agbandje-McKenna, unpublished results). We report the production, purification, crystallization and preliminary X-ray crystallographic analysis of the
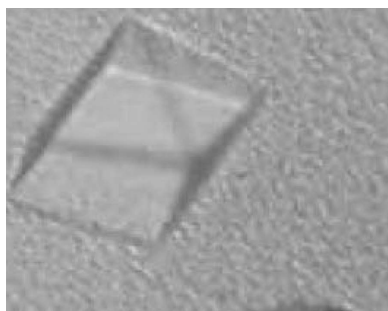
AAV5 viral capsid as a step toward identifying the capsid regions responsible for its cellular transduction and sialic acid binding.

2. Materials and methods

2.1. Production and purification

A recombinant baculovirus encoding the AAV5 viral capsid open reading frame (ORF) was constructed using the Bac-to-Bac system (Gibco BRL). The AAV2 capsid ORF in pFBDVPm11 (Urabe *et al.*, 2002) was replaced by the respective ORF encoding AAV5 capsid proteins derived from pAAV2/5 (Gao *et al.*, 2002). Similar mutations were introduced into 5′-noncoding and coding sequences to enable the expression of the AAV5 capsid proteins in the insect-cell background (Urabe *et al.*, 2002) and the resulting construct expressed all three AAV capsid proteins: VP1, VP2 and VP3. DH10Bac-competent cells containing the baculovirus genome were transformed with pFastBac transfer plasmids containing the AAV component insert. Bacmid DNA purified from recombination-positive white colonies was transfected into Sf9 cells using TransIT Insecta reagent (Mirus). 3 d post-transfection, media containing baculovirus (pooled viral stock) were harvested and a plaque assay was conducted to prepare independent plaque isolates. Several individual plaques were propagated to passage one (P1) to assay for the expression of the AAV5 capsid genes and a selected clone was propagated to P2.

A titered P2 stock was used to infect Sf9 insects grown in Erlenmeyer flasks at 300 K using Sf-900 II SFM media (Gibco/Invitrogen Corporation). The cells were infected at a multiplicity of infection of 5.0 plaque-forming units per cell. The virus capsids were released from the cells by three cycles of rapid freeze–thaw in lysis buffer (50 mM Tris–HCl pH 8.0, 100 mM NaCl, 1 mM EDTA, 0.2% Triton X-100) with the addition of benzonase (Merck KGaA, Germany) in the final cycle. The sample was clarified by centrifugation at 10 000 rev min^{-1} for 15 min at 277 K. The cell lysate was pelleted through a 20%(w/v) sucrose cushion by ultracentrifugation at 45 000 rev min^{-1} for 3 h at 277 K. The pellet from the cushion was resuspended overnight with stirring at 277 K in lysis buffer. The resuspended sample was subjected to a low-speed 2000 rev min^{-1} spin to remove particulate material and further purified with two rounds of sucrose-step gradients [5–40%(w/v)] by ultracentrifugation at 35 000 rev min^{-1} for 3 h at 277 K. A visible blue fraction containing empty (no DNA) viral capsids, sedimenting at ∼25% sucrose, was extracted after the second gradient and dialyzed against 20 mM Tris–HCl pH 8.5 containing 250 or 350 mM NaCl by stirring overnight at 277 K. The approximate concentrations of the samples were calculated from optical density measurements, assuming an extinction coefficient of 1.7 for calculations in mg ml^{-1}. The concentrations were adjusted to ∼11 mg ml^{-1} using Centricon filters (Amicon Centricons, 100 000 molecular-weight cutoff) at 3000 rev min^{-1} and 277 K. The purity and integrity of the viral capsids were monitored using SDS–gel electrophoresis and negative-stain electron microscopy, respectively.

2.2. Electron microscopy

Purified AAV5 viral capsids were viewed using a Joel JEM-100CX II electron microscope (EM). 5 µl purified virus solution at an estimated concentration of 2.0 mg ml^{-1} was spotted onto a 400 mesh carbon-coated copper grid (Ted Pella, Inc., Redding, CA, USA) for 1 min before blotting with filter paper (Whatman No. 5). The sample was then negatively stained with 5 µl 2% uranyl acetate for 17 s, blotted dry and viewed.

2.3. Crystallization

Based on reports for AAV4 (Kaludov *et al.*, 2003) and AAV8 (Lane *et al.*, 2005) viral capsids, AAV5 crystallization conditions were screened against precipitant solutions containing varying polyethylene glycol (PEG) 8000 (0.5–2.5%), NaCl (250 and 350 mM) and MgCl$_2$ (5–20 mM) concentrations and a pH range (pH 6.0–8.5) at room temperature (RT) and 277 K. A buffer concentration of 20 mM for both Bis-Tris (pH 6.0 and 6.5) and Tris–HCl (pH 7.0–8.5) was used for the pH screens. The crystal screens were set up using the hanging-drop vapor-diffusion method (McPherson, 1982) with VDX 24-well plates and siliconized cover slips (Hampton Research, Laguna Niguel, CA, USA). The crystallization drops contained 2 µl sample solution (at ∼11 mg ml^{-1}) and 2 µl precipitant solution equilibrated against 1 ml precipitant solution.

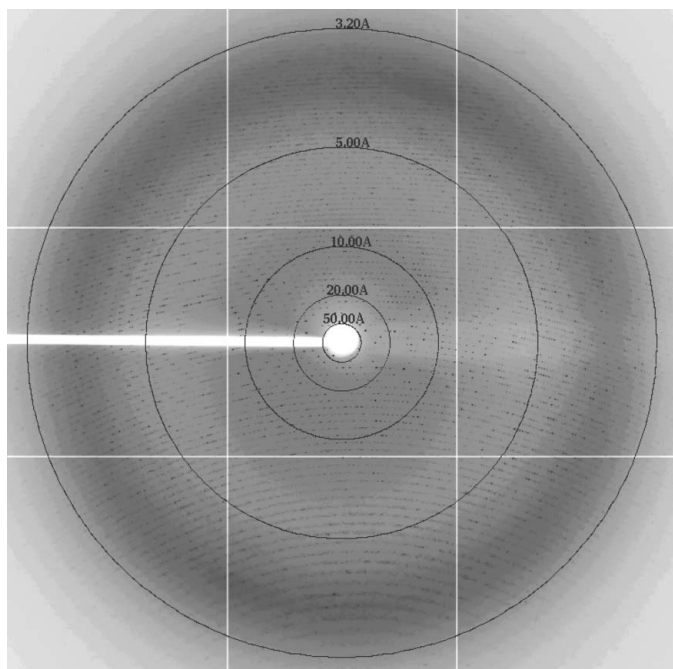### 2.4. Data collection and reduction

X-ray diffraction data were collected from crystals that were cryoprotected with 30% glycerol in the precipitant solution containing 5% PEG 8000 and flash-frozen in a nitrogen stream. Diffraction images were collected at the X29 beamline at the National Synchrotron Light Source (NSLS, Brookhaven National Laboratory) at λ = 1.100 Å on an ADSC Quantum Q315 CCD detector and at the F1 station at the Cornell High Energy Synchrotron Source (CHESS, Cornell University) at λ = 0.924 Å on an ADSC Quantum 4 CCD detector. Crystal-to-detector distances of 300–400 mm were used to record 0.3° oscillation images at exposure times of 30–60 and 360 s on the X29 and F1 beamlines, respectively. The measured diffraction intensities were indexed, integrated, scaled and merged with the *HKL*2000 suite of programs (*DENZO* and *SCALEPACK*; Otwinowski & Minor, 1997). The intensity data set was converted to structure-factor amplitudes using the *TRUNCATE* program from *CCP*4 (Collaborative Computational Project, Number 4, 1994).
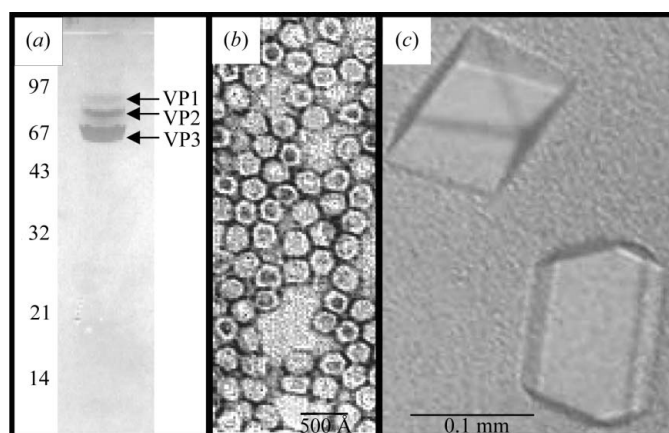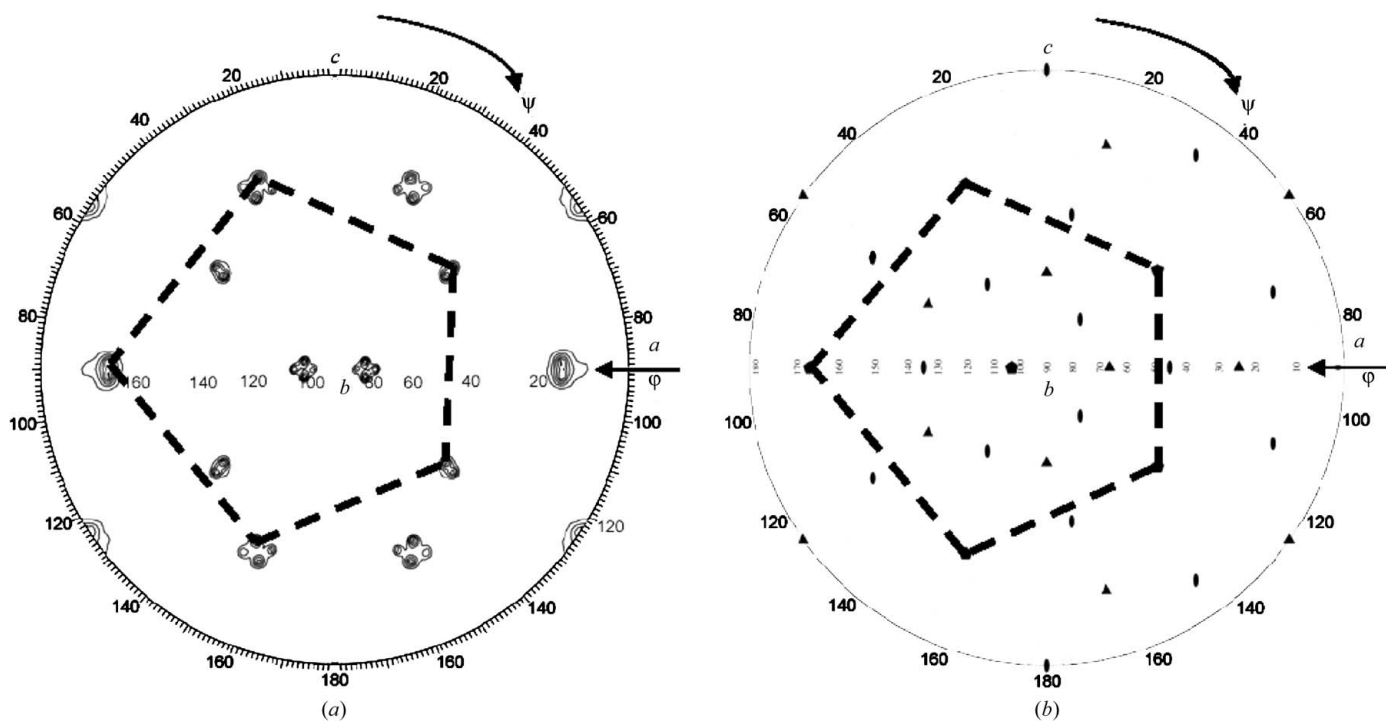

Figure 1
Isolation and characterization of purified AAV5 empty viral capsids. (*a*) SDS–PAGE gel of AAV5 showing the positions of VP1, VP2 and VP3, which are 80, 65 and 59 kDa in size, respectively. The expected positions for low-molecular-weight standards (in kDa; Bio-Rad, Hercules, CA, USA) are indicated on the right-hand side. (*b*) Transmission electron micrograph of purified AAV5 empty (no DNA) viral capsids negatively stained with 2% uranyl acetate (UA). The dark centers indicate the uptake of UA into the empty capsids. (*c*) Optical photograph of AAV5 empty viral capsid crystals. Crystals are ∼0.15 × 0.10 × 0.05 mm in size. The photograph was taken with a Bio-Rad 1024 ES confocal microscope with an Olympus IX 70 transmission.

2.5. Calculation of particle orientations and positions

The orientations of the AAV5 viral capsids in the crystal unit cell were determined by computing a self-rotation function (Tong & Rossmann, 1997) using the *GLRF* program. The calculations used ~10% of the observed reflections between 10.0 and 4.0 Å with the largest amplitudes to represent the second Patterson. The radius of integration was 120 Å, with κ = 72, 120 and 180° to search for fivefold, threefold and twofold non-crystallographic symmetry (NCS) elements of the icosahedral virus capsid. A polyalanine model of the AAV4 VP3 crystal structure (Govindasamy *et al.*, unpublished results) was generated by the *MOLEMAN* program (Kleywegt *et al.*, 2001) and used as a model for cross-rotation and translation-function searches using the *AMoRe* program (Navaza, 1994).

3. Results and discussion

3.1. Crystallization

The purity and integrity of the empty AAV5 viral capsids were verified by SDS–PAGE (Fig. 1*a*) and negative-stain EM (Fig. 1*b*), respectively, prior to crystallization. Crystals of the AAV5 viral capsids that were ~0.15 × 0.10 × 0.05 mm in size were obtained in ~2–3 weeks in 350 m*M* NaCl, 2–20 m*M* MgCl$_2$, 1.5% PEG 8000 and pH 6.0–8.0 at RT. The screens set up at 277 K produced crystals of similar size after ~9 months of incubation (Fig. 1*c*). Crystals grown in 20 m*M* Tris–HCl pH 7.5, 350 m*M* NaCl, 5–10 m*M* MgCl$_2$, 1.5% PEG 8000 at RT and in 20 m*M* Tris–HCl pH 8.5, 350 m*M* NaCl, 10 m*M* MgCl$_2$, 1.5% PEG 8000 at 277 K have been used for data collection.

3.2. Data collection, processing and scaling

The crystals diffracted X-rays to beyond 3.2 Å resolution (Fig. 2). The data were indexed in a primitive orthorhombic crystal system, with unit-cell parameters a = 264.7, b = 447.9, c = 629.7 Å (Table 1). Inspection of the *h*00, 0*k*0 and 00*l* classes of reflections showed systematic absences for the odd reflections, indicating that there were

Figure 2
X-ray diffraction image for a crystal of AAV5 empty (no DNA) viral capsids. The image is a 0.3° oscillation diffraction pattern collected at the X29 (NSLS, BNL) beamline. The crystals diffract X-rays to beyond 3.2 Å resolution. Concentric rings depict the 50.0, 20.0, 10.0, 5.0 and 3.2 Å resolution shells.

Figure 3
Stereographic projections of the AAV5 empty (no DNA) viral capsid orientations determined by rotation-function calculations. (*a*) The self-rotation function for κ = 72° showing fivefold icosahedral symmetry elements (of the four capsids) in the crystal unit cell. The search used observed data in the 10–4.0 Å resolution range, with a radius of integration of 120 Å. The rotation function is contoured at 1σ intervals and the peaks belonging to one viral capsid are outlined in the dashed pentagon. (*b*) The positions of the icosahedral twofold, threefold and fivefold axes for one capsid. The fivefold peaks for the capsid are outlined as in (*a*).

crystallization communications

three mutually perpendicular 2_1 screw axes and that the crystals belong to space group $P2_12_12_1$. The data collected from the crystals grown at RT scale with an overall R_{sym} of 16.1% (Table 1), while the data from the crystals grown at 277 K have high scaling statistics ($R_{merge} > 25\%$), possibly owing to radiation damage to the small crystals during data collection. Thus, only the data collected on crystals grown at RT were usable. The statistics for this data set are given in Table 1.

The unit-cell parameters and the molecular weight of the AAV5 empty viral capsid gave a V_M value (Matthews, 1968; Kantardjieff & Rupp, 2003) of 5.2 Å^3 Da^{-1} for one capsid per asymmetric, corresponding to a solvent content of $\sim$76%, assuming a molecular density of 1.3 g cm^{-3}. The high V_M is likely to be a consequence of the crystals being formed from empty viral capsids and thus containing a shell of protein surrounding solvent. If the center of the capsid was occupied by the genomic DNA, the V_M value (3.6 Å^3 Da^{-1}) would be within the range for protein–nucleic acid complexes (Kantardjieff & Rupp, 2003).

3.3. Molecular replacement: particle orientation and position determinations

The orientation of the AAV5 viral capsid in the asymmetric unit cell was determined with a self-rotation function (Tong & Rossmann, 1997) that searched for the twofold, threefold and fivefold icosahedral symmetry axes of the virus capsid with $\kappa = 180$ (Fig. 3a), 120 and 72°, respectively. Each peak within the rotation function was split into four, showing the orientations for all four crystallographic symmetry-related viral capsids in the unit cell (Fig. 3a). A cross-rotation function calculated with the *AMoRe* program (Navaza, 1994) using a AAV4 polyalanine model (Govindasamy *et al.*, unpublished results) gave Eulerian angles of $\alpha = 107.5$, $\beta = 33.8$, $\gamma = 55.1°$ for rotating the model in the standard icosahedral orientation, as defined by Rossmann *et al.* (1992), onto one of the AAV5 viral capsid orientations in the crystal unit cell (Fig. 3b). A translation-function search with the oriented AAV4 model, also using the *AMoRe* program, gave the lowest R factor of 53.9% and highest correlation coefficient (CC) of 0.26 for the asymmetric unit capsid positioned at fractional coordinates (0.3241, 0.2645, 0.3234) for data in the 10.0–6.0 Å resolution range. Rigid-body refinement (FITTING in *AMoRe*) of the orientated and positioned model improved the R factor and CC to 44.7% and 0.53, respectively.

The structure determination of the AAV5 viral capsid to 3.45 Å resolution is currently in progress using the molecular-replacement solution and initial phases calculated with the AAV4 polyalanine model (Govindasamy *et al.*, unpublished results). A comparison of the crystal structure of AAV5 with those available for AAV2 (Xie *et al.*, 2002) and AAV4 (Govindasamy *et al.*, unpublished results) and the pseudo-atomic model of AAV5 VP3 built into the cryo-electron microscopy image reconstructed density of AAV5 (Walters *et al.*, 2004) will provide the necessary information for further analyzing the structural determinants of cellular transduction specificities with the aim of improving the efficacy of rAAVs for targeted gene-therapy applications.

References

Bantel-Schaal, U., Delius, H., Schmidt, R. & zur Hausen, H. (1999). *J. Virol.* **73**, 939–947.

Burger, C., Gorbatyuk, O. S., Velardo, M. J., Peden, C. S., Williams, P., Zolotukhin, S., Reier, P. J., Mandel, R. J. & Muzyczka, N. (2004). *Mol. Ther.* **10**, 302–317.

Collaborative Computational Project, Number 4 (1994). *Acta Cryst.* D**50**, 760–763.

Davidson, B. L., Stein, S. C., Heth, J. A., Martins, I., Kotin, R. M., Derksen, T. A., Zabner, J., Ghodsi, A. & Chiorini, J. A. (2000). *Proc. Natl Acad. Sci. USA*, **97**, 3428–3423.

Flotte, T. R. & Carter, B. J. (1995). *Gene Ther.* **2**, 357–362.

Gao, G. P., Alvira, M. R., Wang, L., Calcedo, R., Johnston, J. & Wilson, J. M. (2002). *Proc. Natl Acad. Sci. USA*, **99**, 11854–11859.

Kaludov, N., Brown, K. E., Walters, R. W., Zabner, J. & Chiorini, J. A. (2001). *J. Virol.* **75**, 6884–6893.

Kaludov, N., Padron, E., Govindasamy, L., McKenna, R., Chiorini, J. A. & Agbandje-McKenna, M. (2003). *Virology*, **306**, 1–6.

Kantardjieff, K. A. & Rupp, B. (2003). *Protein Sci.* **12**, 1865–1871.

Kern, A., Schmidt, K., Leder, C., Muller, O. J., Wobus, C. E., Bettinger, K., Von der Lieth, C. W., King, J. A. & Kleinschmidt, J. A. (2003). *J. Virol.* **77**, 11072–11081.

Kleywegt, G. J., Zou, J. Y., Kjeldgaard, M. & Jones, T. A. (2001). *International Tables for Crystallography*, Vol. *F*, edited by M. G. Rossmann & E. Arnold, pp. 353–356, 366–367. Dordrecht: Kluwer Academic Publishers.

Lane, M. D., Nam, H.-J., Padron, E., Gurda-Whitaker, B., Kohlbrenner, E., Aslanidi, G., Byrne, B., McKenna, R., Nuzyczka, N., Zolotukhin, S. & Agbandje-McKenna, M. (2005). *Acta Cryst.* F**61**, 558–561.

McPherson, A. (1982). *Preparation and Analysis of Protein Crystals*, 1st ed., pp. 96–99. New York: Wiley.

Matthews, B. W. (1968). *J. Mol. Biol.* **33**, 491–497.

Mori, S., Wang, L., Takeuchi, T. & Kanda, T. (2004). *Virology*, **330**, 375–383.

Navaza, J. (1994). *Acta Cryst.* A**50**, 157–163.

Opie, S. R., Warrington, K. H. Jr, Agbandje-McKenna, M., Zolotukhin, S. & Muzyczka, N. (2003). *J. Virol.* **77**, 6995–7006.

Otwinowski, Z. & Minor, W. (1997). *Methods Enzymol.* **276**, 307–326.

Rabinowitz, J. E., Rolling, F., Li, C., Conrath, H., Xiao, W., Xiao, X. & Samulski, R. J. (2002). *J. Virol.* **76**, 791–801.

Rossmann, M. G., McKenna, R., Tong, L., Xia, D., Dai, J., Wu, H., Choi, H. K. & Lynch, R. E. (1992). *J. Appl. Cryst.* **25**, 166–180.

Tong, L. & Rossmann, M. G. (1997). *Methods Enzymol.* **276**, 594–611.

Urabe, M., Ding, C. & Kotin, R. M. (2002). *Hum. Gene Ther.* **13**, 1935–1943.

Walters, R., Agbandje-McKenna, M., Bowman, V. D., Moninger, T. O., Olson, N. H., Seiler, M., Chiorini, J. A., Baker, T. S. & Zabner, J. (2004). *J. Virol.* **78**, 3361–3371.

Walters, R., Yi, S. M., Keshavjee, S., Brown, K., Welsh, M., Chiorini, J. & Zabner, J. (2001). *J. Biol. Chem.* **276**, 20610–20616.

Xie, Q., Bu, W., Bhatia, S., Hare, J., Somasundaram, T., Azzi, A. & Chapman, M. S. (2002). *Proc. Natl. Acad. Sci. USA*, **99**, 10405–10410.